Supporting information

Highly Sensitive 2D Organic Field-effect Transistors for the Detection of Lithium-ion Battery Electrolyte Leakage

Ben Yang, Shiqi Zhang, Yan Wang, Shilei Dai, Xin Wang, Quan Sun, Yunhui Huang* and Jia Huang*

Experimental section

Material synthesis

F15-NTCDI was synthesized according to the previous report, and then purified by vacuum sublimation. F15-NTCDI semiconductor layer (50 nm) was thermally evaporated onto Si wafer with a thermally grown 300 nm SiO_2 layer. Afterward, 40 nm Au was thermally evaporated with the aid of a shadow mask to fabricate the n-type OFETs. The LIB electrolyte we used are commercial electrolyte for lithium batteries (Product Name: LBC305-01), which consist of DMC, DEC, EMC, EC, and LiFP6 etc.

Device fabrication

A heavily n-doped Si wafer with a thermally grown 300 nm SiO_2 layer was used as the substrate. Before the device fabrication, the substrates were sonicated for 30 minutes in acetone and isopropanol, then washed with ethanol and deionized water, and finally dried with N_2. To obtain the 2 nm thick PQT-12 film, PQT-12 solution (1.5 mg PQT-12 dissolved in 1 ml dichlorobenzene) was then spin-coated on the pre-cleaned substrate without OTS at 5000 rpm for 60 s. The films were placed in a vacuum chamber for 10 minutes to remove most of the solvent, and then thermally annealed at 100 ^{o}C for 30 minutes. Afterward, 40 nm Au source/drain electrodes were thermally evaporated through a shadow mask with a channel length of 50 μm and channel width of 7 mm. The control sample with the film thickness of 25 nm was prepared using a PQT-12 solution (4 mg/ml in chlorobenzene) by controlling the spin speed at 1500 rpm for 30 s. For the 110 nm control sample, 10 mg/ml solution was spin-coated onto the substrate at 1000 rpm for 60 s.

Characterization and measurements

Optical image of the OSCs film was investigated by an optical microscope (Shanghai Optical Instrument Factory, 6XB-PC). The micromorphology and thickness of the OSCs film were measured by atomic force microscope (AFM, SEIKO SPA300HV). The electrical properties and sensing performance of the sensors were measured by a Keithley 4200-SCS connected to a 6 L homemade gas chamber.

Figure S1. AFM images of DPP DTT and PDPP4T ultrathin films and their electrical properties. (a) and (b) AFM images of DPP DTT and PDPP4T ultrathin films, respectively. (below: structure of DPP DTT and PDPP4T). (c) and (d) Transfer curves of DPP DTT and PDPP4T ultrathin OFETs, respectively.

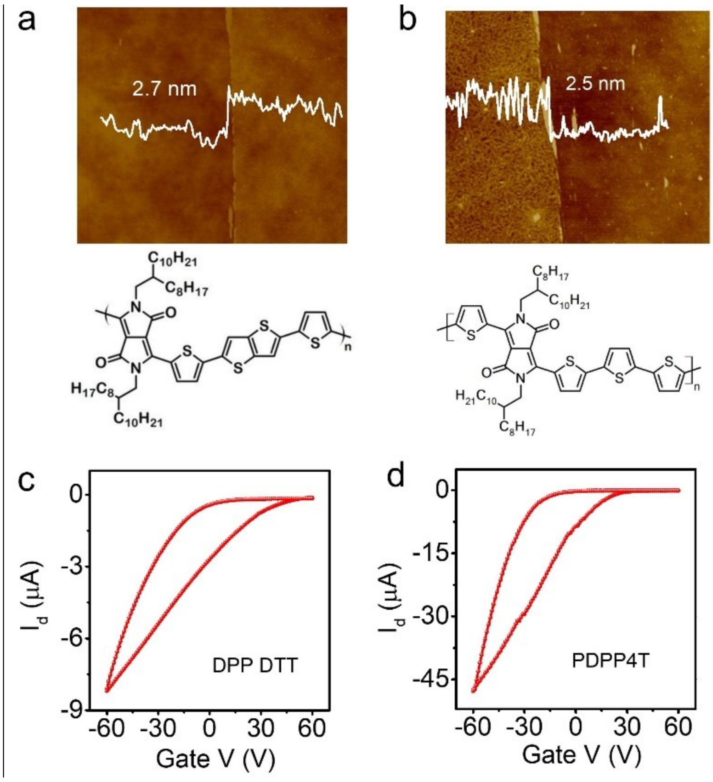

Figure S2. Response of three types of ultrathin film OFETs to 200 ppm DMC vapor.

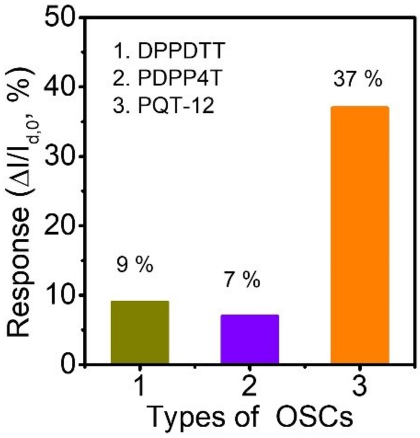

Figure S3. PQT-12 films characterization. (a) Optical image of the 2 nm thick PQT-12 film. (b) and (c) The thickness of the two PQT-12 control films.

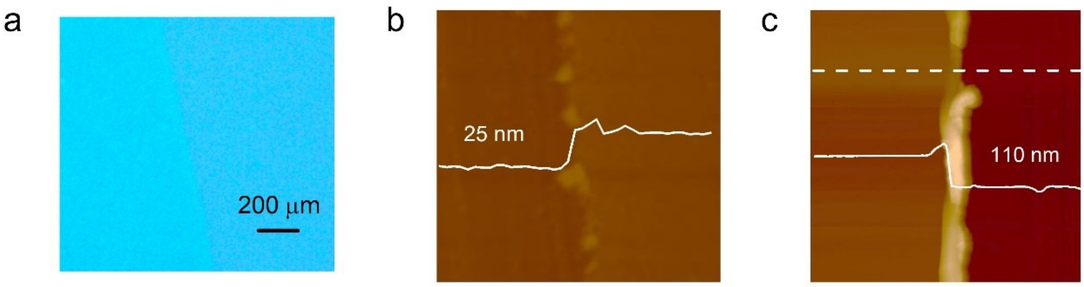

Figure S4. Electrical properties of different thickness PQT-12 OFETs. (a) and (b) Output characteristics of the 25 nm and 110 nm control samples.

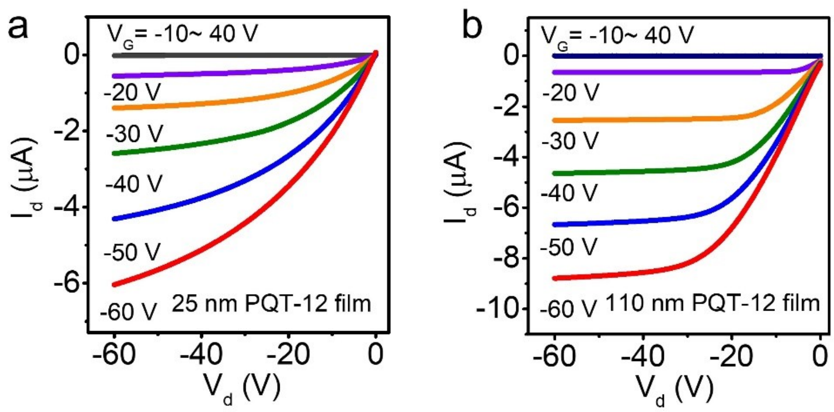

Figure S5. Response and recovery time of the (a) 2 nm, and (b) 25 nm PQT-12 OFETs sensor.

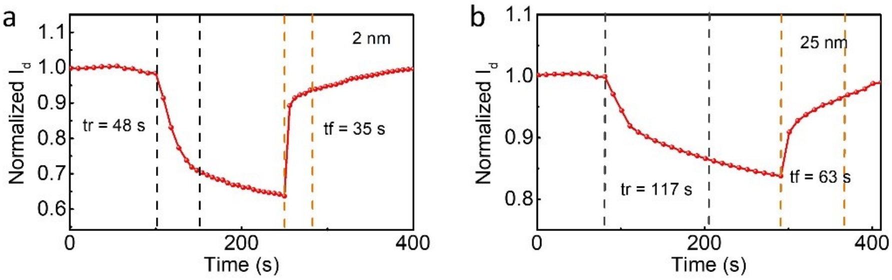

Figure S6. Normalized response of the ultrathin PQT-12 OFETs to DMC vapor at different concentrations.

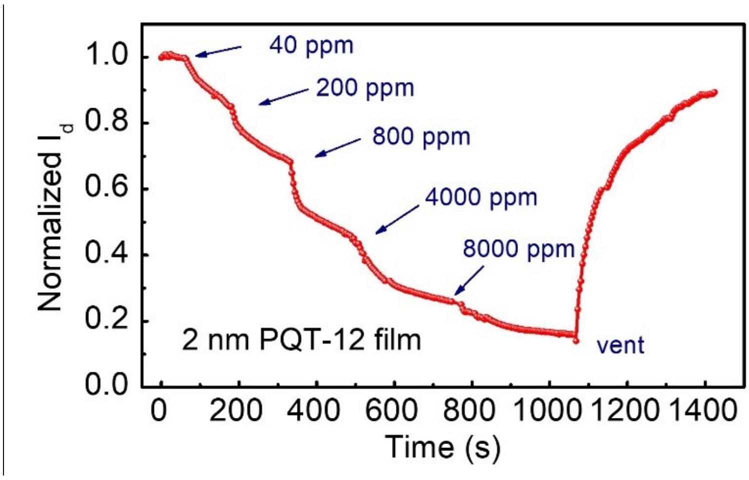

Figure S7. Limit of detection of the ultrathin PQT-12 OFETs. (a) Noise of the 2 nm PQT-12 OFETs. (b) Limit of detection of the ultrathin PQT-12 OFETs toward DMC.

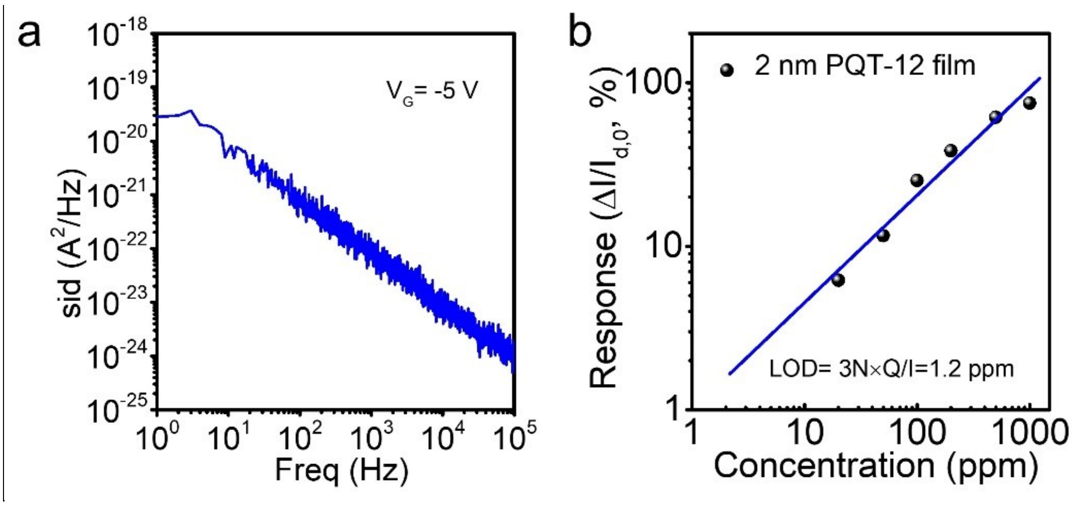

Figure S8. Electrical properties of the n-type F15-NTCDI OFETs. (a) Output characteristic of the F15-NTCDI OFETs. (b) Transfer curves of the F15-NTCDI OFETs.

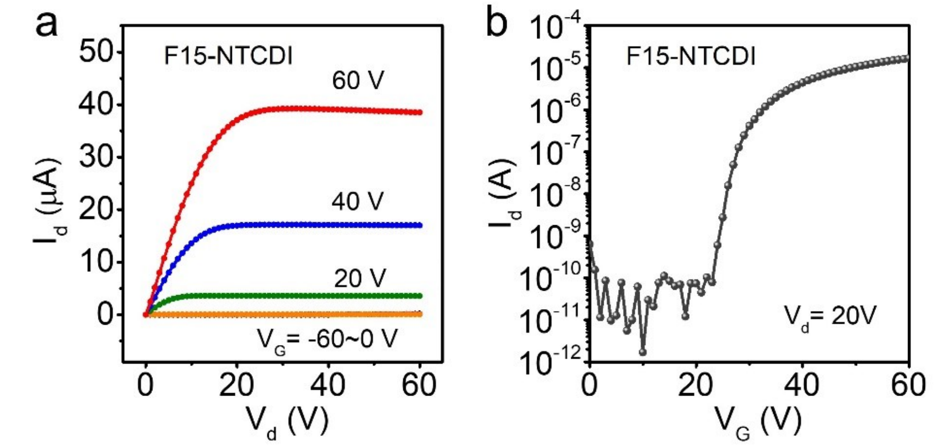

Figure S9. The ultrathin OFETs sensor response to (a) 2000 ppm DMC and (b) 5 ppm DMC.

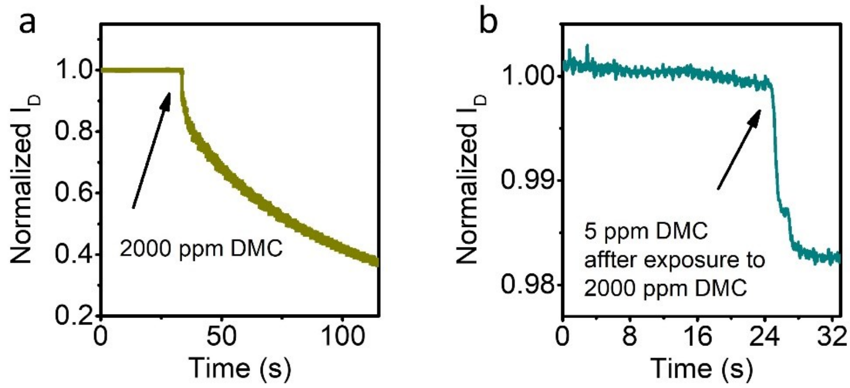

Figure S10. Limit of detection of the 2 nm PQT-12 OFETs toward LIBs electrolyte.

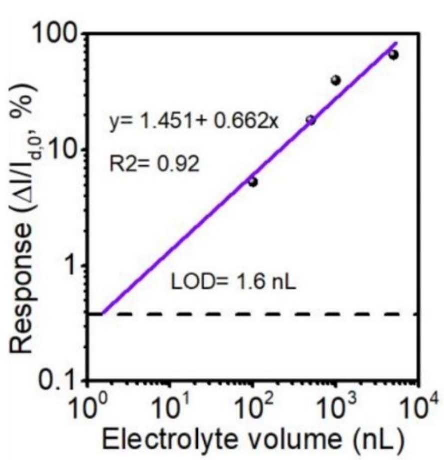

Figure S11. The sensor response to (a) DMC and (b) LIBs electrolyte at low concentrations.

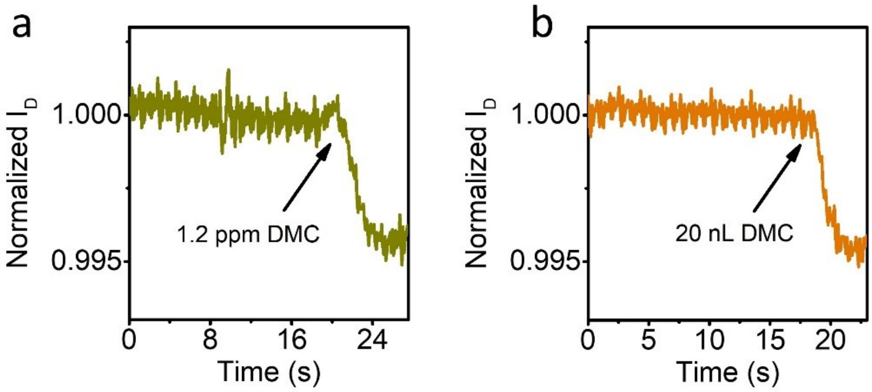

Figure S12. The sensor response to different electrolyte solvents vapors. The ultrathin OFETs sensor response to 10 ppm (a) DMC, (b) EMC and (c) DEC electrolyte vapors.